

Article

Not peer-reviewed version

---

# Luminescence of ZrO<sub>2</sub>: Ti Ceramics Irradiated with High-Energy Xenon Ions

---

[Alma Dauletbekova](#)<sup>\*</sup>, Sergey Zvonarev, Sergey Nikiforov, [Abdirash Akilbekov](#), Tatiana Shtang, Natalia Karavannova, [Aiman Akylbekova](#), [Alexey Ishchenko](#), Gulzhanat Akhmetova-Abdik, Zein Baimukhanov, [Gulnara Aralbayeva](#), [Guldar Baubekova](#), [Anatoli I Popov](#)

Posted Date: 4 October 2023

doi: 10.20944/preprints202310.0158.v1

Keywords: zirconium dioxide; thermoluminescence; pulse cathodoluminescence; ceramics; scanning electron microscopy



Preprints.org is a free multidiscipline platform providing preprint service that is dedicated to making early versions of research outputs permanently available and citable. Preprints posted at Preprints.org appear in Web of Science, Crossref, Google Scholar, Scilit, Europe PMC.

Copyright: This is an open access article distributed under the Creative Commons Attribution License which permits unrestricted use, distribution, and reproduction in any medium, provided the original work is properly cited.

Disclaimer/Publisher's Note: The statements, opinions, and data contained in all publications are solely those of the individual author(s) and contributor(s) and not of MDPI and/or the editor(s). MDPI and/or the editor(s) disclaim responsibility for any injury to people or property resulting from any ideas, methods, instructions, or products referred to in the content.

## Article

# Luminescence of $\text{ZrO}_2$ : Ti ceramics irradiated with high-energy xenon ions

Alma Dauletbekova <sup>1,\*</sup>, Sergey Zvonarev <sup>2</sup>, Sergey Nikiforov <sup>2</sup>, Abdirash Akilbekov <sup>1</sup>, Tatiana Shtang <sup>2</sup>, Natalia Karavannova <sup>2</sup>, Aiman Akylbekova <sup>1</sup>, Alexey Ishchenko <sup>2</sup>, Gulzhanat Akhmetova-Abdik <sup>1</sup>, Zein Baymukhanov <sup>1</sup>, Gulnar Aralbayeva <sup>1</sup>, Guldar Baubekova <sup>1</sup> and Anatolii I. Popov <sup>3</sup>

<sup>1</sup> Department of Technical Physics, L.N. Gumilyov Eurasian National University, Satpayev Str. 2, Astana 010008, Kazakhstan, alma\_dauletbek@mail.ru (A.D.), akilbekov\_at@enu.kz (A.A.), aiman88\_88@mail.ru (A.A.), gulzhanatakhmet@gmail.com (G.A-A.), zeinb77@mail.ru (Z.B.), agm\_555@mail.ru (G.A.), guldar\_87@mail.ru (G.B.).

<sup>2</sup> Ural Federal University, 19 Mira str., Yekaterinburg, 620002, RF, s.v.zvonarev@urfu.ru (S.Z.), s.v.nikiforov@urfu.ru (S.N.), T.v.shtang@urfu.ru (T.S.), Natalia.Karavannova@urfu.me (N.K.), A.v.ishchenko@urfu.ru (A.I.)

<sup>3</sup> Institute of Solid State Physics, University of Latvia, Kengaraga 8, LV-1063 Riga, Latvia; anatoli.popov@cfi.lu.lv (A.P.)

\* Correspondence: alma\_dauletbek@mail.ru

**Abstract:** Samples of  $\text{ZrO}_2$  ceramics with different concentrations of impurity titanium ions were synthesized by mixing powders of zirconium and titanium oxides in various mass ratios. The phase composition and surface morphology of the studied ceramics were determined by X-ray phase analysis and scanning electron microscopy. It was found that irradiation of samples with xenon ions (220 MeV) with fluences  $10^{10}$  and  $10^{12}$   $\text{ion/cm}^2$  leads to a decrease in the intensity of the pulse cathodoluminescence band at 2.5 eV. It is shown that ion irradiation causes the appearance of a new peak of thermoluminescence at 450-650 K of a non-elementary form associated with radiation-induced traps of charge carriers. In contrast to electron irradiation, an increase in the fluence of ions leads to a decrease in the intensity of this peak. In contrast to electron irradiation, an increase in the fluence of ions leads to a decrease in the intensity of this peak. A complex nonmonotonic dependence of the cathode and thermoluminescence intensity on the dopant concentration was found, which may be due to the effects of concentration quenching and aggregation of defective centers.

**Keywords:** zirconium dioxide; thermoluminescence; pulse cathodoluminescence; ceramics; scanning electron microscopy

## 1. Introduction

Zirconium dioxide ( $\text{ZrO}_2$ ) has a high refractive index, thermal and chemical stability, which allows it to be used in many industries, in particular as heat-shielding coatings, electron-optical materials and ionizing radiation detectors [1]. There are different types of detectors, with luminescent detectors and thermoluminescent dosimeters being notable examples. Thermoluminescence dosimetry (TLD) involves the use of crystals or ceramics with specific lattice defects of impurity and/or intrinsic origin, known as crystal phosphors. These substances can emit light when exposed to ionizing radiation and subsequently heated. In this case, the amount of ionizing radiation absorbed is directly proportional to the number of emitted quanta [2]. TL-dosimetry is widely used for individual dosimetry of personnel, environmental monitoring, and medical exposure control. Thermoluminescent detectors use a variety of materials, such as alkaline-halides ( $\text{LiF}$ : Mg, Ti;  $\text{LiF}$ : Mg, Cu, P), sulphates ( $\text{BaSO}_4$ : Eu,  $\text{CaSO}_4$ : Dy), borates ( $\text{MgB}_4\text{O}_7$ : Dy), oxides ( $\text{Al}_2\text{O}_3$ ,  $\text{ZnO}$ ,  $\text{ZrO}_2$ ,  $\text{MgO}$ ), and complex compounds ( $\text{K}_3\text{Na}(\text{SO}_4)_2$ : Eu,  $\text{Ba}_{0.97}\text{Ca}_{0.03}\text{SO}_4$ : Eu, YAG etc.) [3–28].

It is known that the luminescent properties of nominally pure and doped zirconium dioxide  $\text{ZrO}_2$  depend on the method of preparation, grain size, crystal structure and morphology of the samples [29–40]. Nominally pure  $\text{ZrO}_2$  is characterized by its own luminescence at 2.5–2.7 eV (470–



490 nm) [29,30,35,38]. According to one point of view, the indicated luminescence band in  $\text{ZrO}_2$  is due to the relaxation of centers associated with intrinsic defects in the anionic sublattice (oxygen vacancies) [30,31,35]. An alternative point of view connects the origin of the luminescence band at 2.6 eV with the relaxation of impurity ions of titanium [32,34,36].

It is known that the introduction of titanium as a dopant can significantly change the luminescent properties of zirconium dioxide. Thus, doping with titanium (0.5 mol%) of nanostructured  $\text{ZrO}_2$  samples led to an increase in photoluminescence (PL) at 480 nm, excited by UV radiation [36]. A similar pattern with increasing dopant amount for the above PL band was observed by other authors. In this case, the maximum intensity was achieved at a titanium concentration of 0.15 weight % [32]. At higher concentrations, a drop in PL was recorded. A similar increase in thermoluminescence (TL) intensity was also discovered when  $\text{ZrO}_2$  was doped with titanium (0.1 mol%) [41,42].

The study of the role of titanium impurities in the formation of the luminescent properties of zirconium dioxide irradiated with high-energy ions, in particular, heavy xenon ions, is of particular interest. It is known that under such irradiation new radiation-induced defects and their complexes are formed in oxide dielectrics [43,44]. These complexes can include both oxygen vacancies and impurity ions in different charge states. It was shown in [45] that complex defects containing oxygen vacancies and titanium ions may be responsible for the formation of the luminescence band at 2.6 eV. In this work, these defects were formed by high-temperature annealing of nominally pure nanostructured zirconium dioxide compacts in vacuum under reducing conditions provided by the presence of carbon in the form of graphite. It can be assumed that such vacancy-impurity complexes can also be generated in samples pre-doped with titanium as a result of high-intensity ion irradiation. In this case, it is of interest to establish the patterns of influence of the concentration of the introduced titanium impurity on the luminescence intensity of samples subjected to such irradiation. In practical terms, such information will be useful for the development of luminescent detectors of ion radiation.

The purpose of this work is to synthesize samples of  $\text{ZrO}_2$  ceramics with different dopant concentrations and evaluate the effect of titanium impurities on the luminescent properties of samples irradiated with xenon ions.

## 2. Materials and Methods

The studied samples were obtained by mixing zirconium and titanium dioxides in the following ratios ( $\text{ZrO}_2:\text{TiO}_2$ ): 99.9:0.1; 99:1; 95:5; 90:10 and 85:15 wt.%. A 99.1% purity zirconium dioxide nanopowder with a particle size in the range of 30-70 nm was used as the starting materials obtained by plasma chemical method (Plasmotherm Company, Russia), and titanium dioxide powder (purity 99.8%, Component Reagent company, Russia). Mixing of the powders was carried out using the dry method in an agate mortar with a binder (ethyl alcohol). The mixing time was 1-2 hours for a quantity of powder weighing 2 g for better homogenization to a dry consistency. Samples in the form of disks were obtained from a mixture of powders (100 mg for each compound) by cold uniaxial pressing at a pressure of 500 MPa. The diameter of the resulting compacts was 6 mm, and the thickness was 1-1.5 mm. Compressed pellets were annealed in air in a high-temperature furnace Linn High Therm HT-1800-M at a temperature of 1200 °C for 1 hour. The selected mode made it possible to ensure the mechanical strength of the samples. Also, in this case, the formation of the  $\text{ZrTiO}_4$  phase did not occur, in the presence of which the luminescence intensity sharply decreased. In this way, samples of  $\text{ZrO}_2:\text{Ti}$  ceramics with different dopant concentrations were obtained.

The luminescent properties of ceramics were studied using pulsed cathodoluminescence (PCL) and TL methods. To excite TL, the studied samples were irradiated with xenon ions with an energy of 220 MeV (fluences of  $10^{10}$  and  $10^{12}$  ions/cm<sup>2</sup>) at the DS-60 heavy ion accelerator (Astana, Republic of Kazakhstan). To carry out a comparative analysis of luminescent properties, the samples were also irradiated with a pulsed electron beam (60 A/cm<sup>2</sup>, 2 ns) from the RADAN EXPERT accelerator with an electron energy of 130 keV at room temperature. The electron irradiation dose was 1.5 kGy per pulse. This electronic radiation, unlike ion radiation, does not lead to the formation of new radiation-induced defects in the material under study, but only changes the charge state of existing ones. The electron beam described above was also used to excite PCL. TL was measured in linear heating mode at a rate of 2 K/s. To register TL, a FEU-130 with a maximum spectral sensitivity of 400-420 nm was used.

### 3. Results

The phase composition and crystal structure of the ceramic samples were determined by X-ray diffraction (XRD) on a Rigaku MiniFlex 600 diffractometer using Cu K $\alpha$ -radiation (wavelength 1.5406 Å, scanning speed 0.3 O/min). Phase identification was conducted using an ICDD PDF-2 database with further Rietveld refinement analysis via the FullProf software.

The resulting diffraction patterns are shown in Figure 1. It can be seen that with the selected synthesis parameters in ceramics with the amount of introduced titanium dioxide of 10% or less, only two phases are observed: baddeleyite (monoclinic ZrO<sub>2</sub>) and tazheranite ((Zr, Ti, Ca) O<sub>2-x</sub>). In this case, the baddeleyite phase predominated for all samples, and its amount was more than 90%. The figure shows the most characteristic reflexes for this phase. In samples with an amount of introduced titanium dioxide of 15%, the rutile phase (TiO<sub>2</sub>) was also recorded in a quantitative content of less than 5%. The inset in Figure 1 shows the most intense diffraction peak belonging to rutile. The crystal lattice parameters of the above phases are given in Table 1.

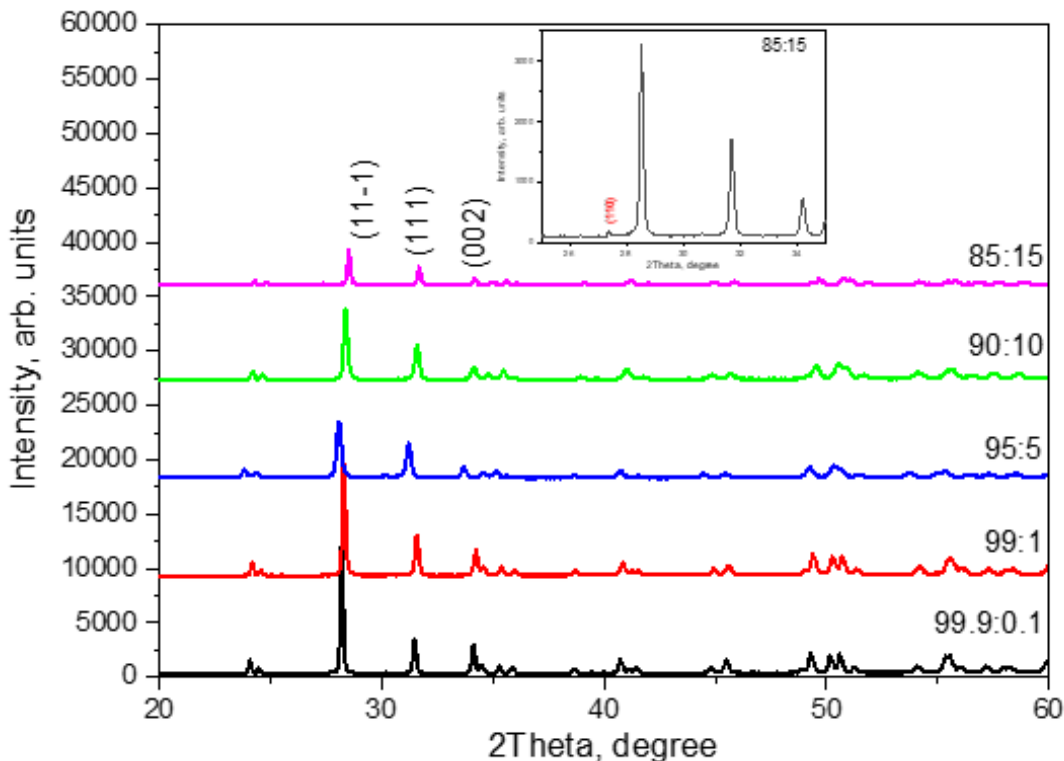
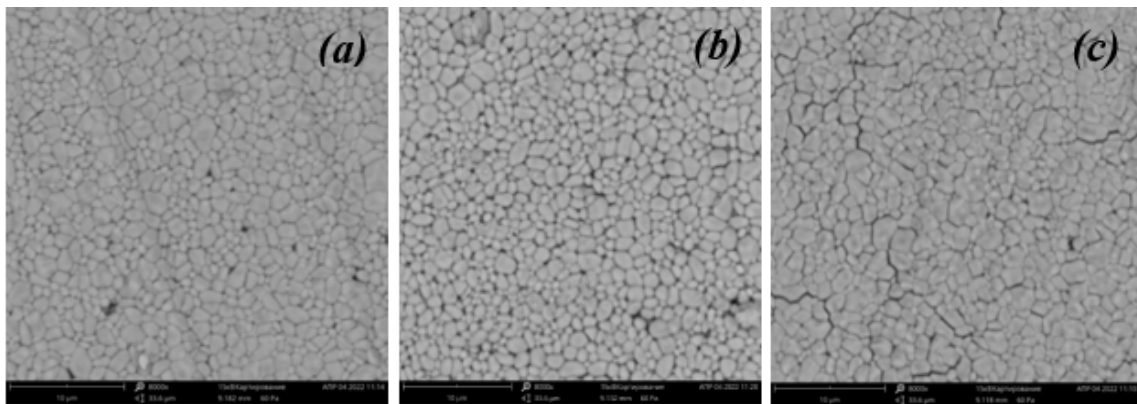


Figure 1. X-ray diffraction patterns of synthesized ceramics with different dopant concentrations.

Table 1. Parameters of crystal lattices of various phases in the samples under study.

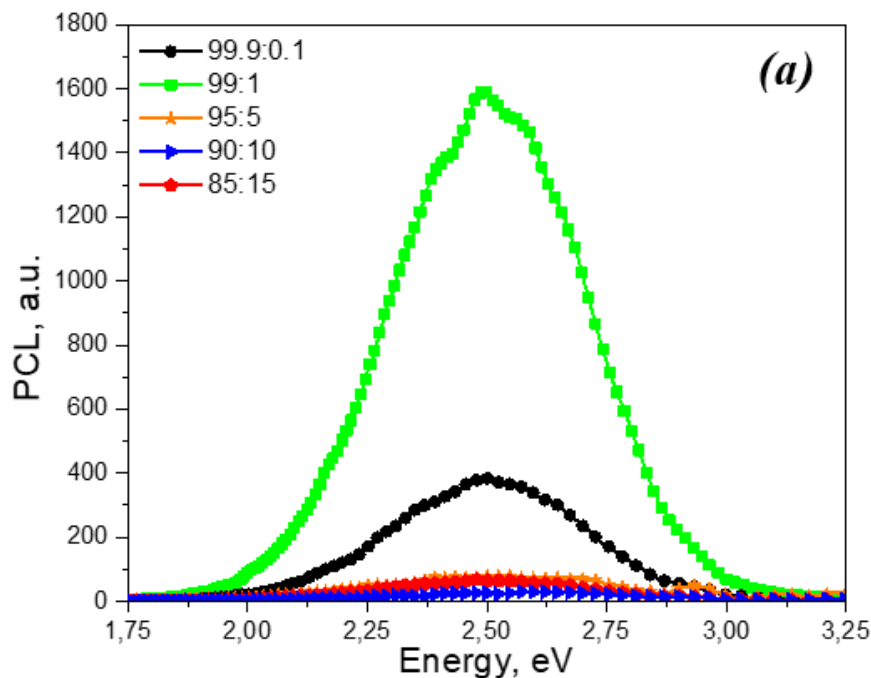
| Phase name                            | Singonia   | a, Å   | b, Å   | c, Å   | $\alpha$ , ° | $\beta$ , ° | $\gamma$ , ° |
|---------------------------------------|------------|--------|--------|--------|--------------|-------------|--------------|
| Baddeleyite (ZrO <sub>2</sub> )       | Monoclinic | 5.1453 | 5.2002 | 5.3236 | 90.000       | 99.094      | 90.000       |
| Tazheranit (Zr,Ti,Ca)O <sub>2-x</sub> | Cubic      | 5.092  | 5.092  | 5.092  | 90.000       | 90.000      | 90.000       |
| Rutile (TiO <sub>2</sub> )            | Tetragonal | 4.6063 | 4.6063 | 2.9773 | 90.000       | 90.000      | 90.000       |

Using a scanning electron microscope, images of the surface of the studied ceramics with different contents of introduced titanium dioxide were obtained (Figure 2). It can be seen that the resulting ceramics have a small number of pores and grains of micron and submicron size. From the analysis of SEM images, we can conclude that all samples are characterized by two groups of grain sizes (0.2-0.5  $\mu$ m and 1-2  $\mu$ m). The sample with a mass fraction of introduced titanium dioxide of 5% has the largest grains (more than 1  $\mu$ m), and the sample with the largest amount of introduced titanium dioxide (15%) has the densest packing among all the ceramics studied.



**Figure 2.** SEM images of synthesized ZrO<sub>2</sub>: Ti ceramics with different percentages of components introduced during synthesis: (a) ZrO<sub>2</sub>:TiO<sub>2</sub> (85:15), (b) ZrO<sub>2</sub>:TiO<sub>2</sub> (90:10) and (c) ZrO<sub>2</sub>:TiO<sub>2</sub> (95:5).

Figure 3 shows the PCL spectra of unirradiated ZrO<sub>2</sub>: Ti ceramics with different dopant concentrations, as well as samples irradiated with xenon ions with fluences of 10<sup>10</sup> and 10<sup>12</sup> ions/cm<sup>2</sup>. It can be seen that all spectra contain one broad band with a maximum at 2.5 eV. In this case, irradiation with xenon ions does not lead to the appearance of new PCL bands. At the same time, in samples irradiated with ions, a decrease in PCL intensity is observed compared to unirradiated samples with the same dopant concentration. The dependence of the maximum luminescence intensity in the 2.5 eV band on the titanium concentration is non-monotonic. The highest PCL intensity in this band is characterized by samples with a concentration of introduced titanium dioxide of 1%. For ceramics with a higher content of introduced titanium dioxide (5 and 10%), this band is characterized by extremely low intensity. At a titanium dioxide concentration of 15%, a slight increase in PCL is observed at 2.5 eV.



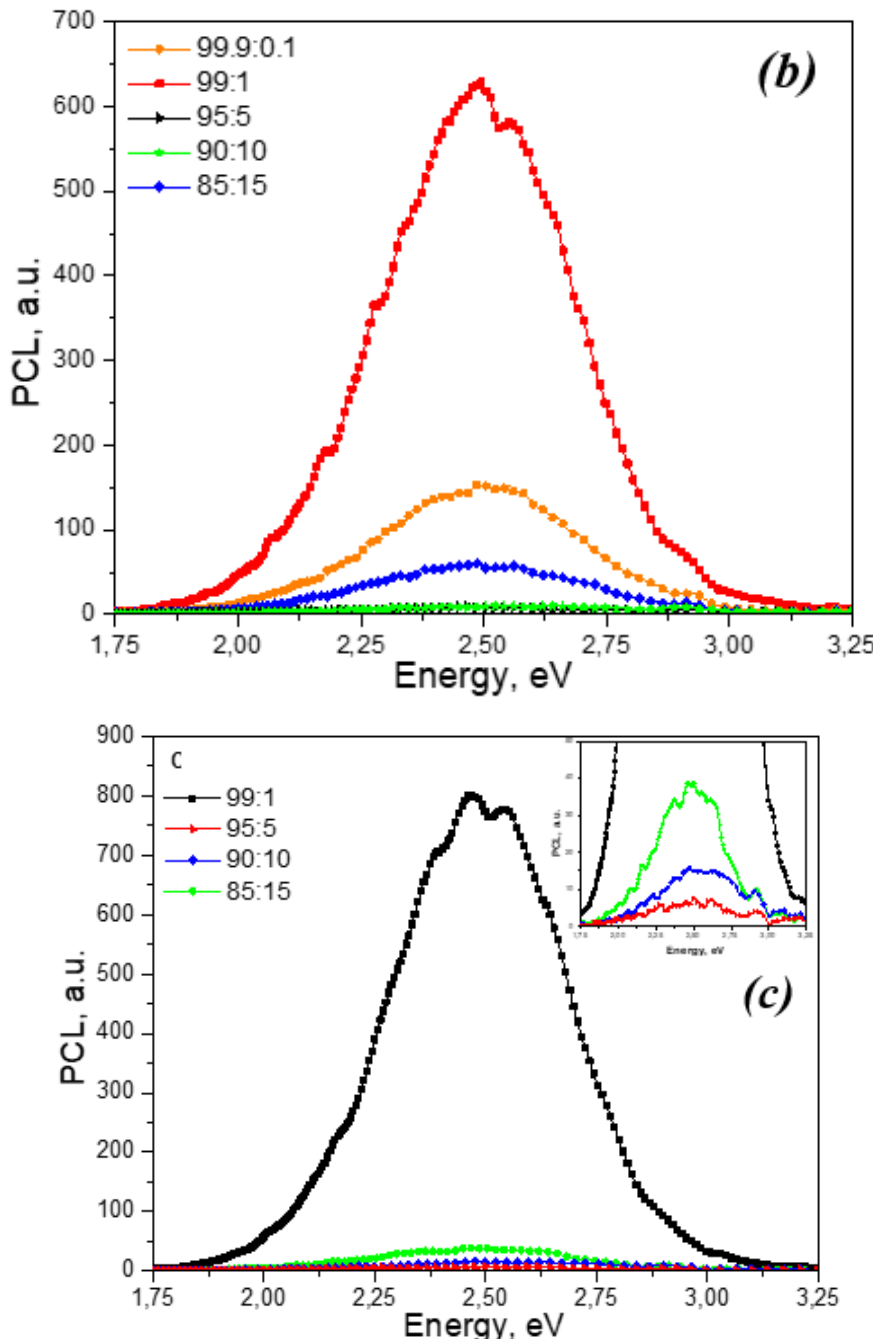


**Figure 3.** PCL spectra of various samples of unirradiated  $\text{ZrO}_2:\text{Ti}$  ceramics (a) and ceramics irradiated with xenon ions with a fluence of  $10^{10}$  ions/ $\text{cm}^2$  (b) and  $10^{12}$  ions/ $\text{cm}^2$  (c).

Figure 4 shows the TL curves of  $\text{ZrO}_2:\text{Ti}$  ceramics corresponding to concentrations of introduced titanium dioxide of 5 and 10%, irradiated with various sources: xenon ions with fluences of  $10^{10}$  and  $10^{12}$  ions/ $\text{cm}^2$  and a pulsed electron beam with doses of 3 and 15 kGy. For samples irradiated with electrons, an intense TL signal is observed at 350-450 K. Moreover, with increasing irradiation dose (from 3 to 15 kGy), its intensity increases.

The TL curves of the same samples irradiated with xenon ions differ significantly from the curves of electron-irradiated samples. Low-temperature TL at 350-450 K is characterized by extremely low intensity, and a new high-temperature TL signal appears at 450-650 K. This signal may be associated with the appearance of new radiation-induced defects as a result of ion irradiation, which play the role of charge carrier traps. The possibility of creating such defects was proven in [46] based on the results of studying EPR spectra. From Figure 4 it is clear that the TL curve at 450-650 K has a non-elementary shape and is a superposition of several TL peaks. This is also evidenced by the

change in the temperature of the TL maximum with variations in the dopant concentration and ion fluence. In this case, with increasing fluence of ion irradiation, a drop in TL intensity is observed at 450-650 K. This pattern was observed for all samples with different concentrations of introduced TiO<sub>2</sub> (from 0.1 to 15%). In this case, the decrease in TL intensity with increasing ion fluence may be associated with radiation destruction of the luminescence centers responsible for TL and the formation of more complex defects. A similar effect of a decrease in the TL yield with increasing ion energy density was observed, in particular, in aluminum oxide single crystals irradiated with pulsed C<sup>+</sup>/H<sup>+</sup> ions [47].

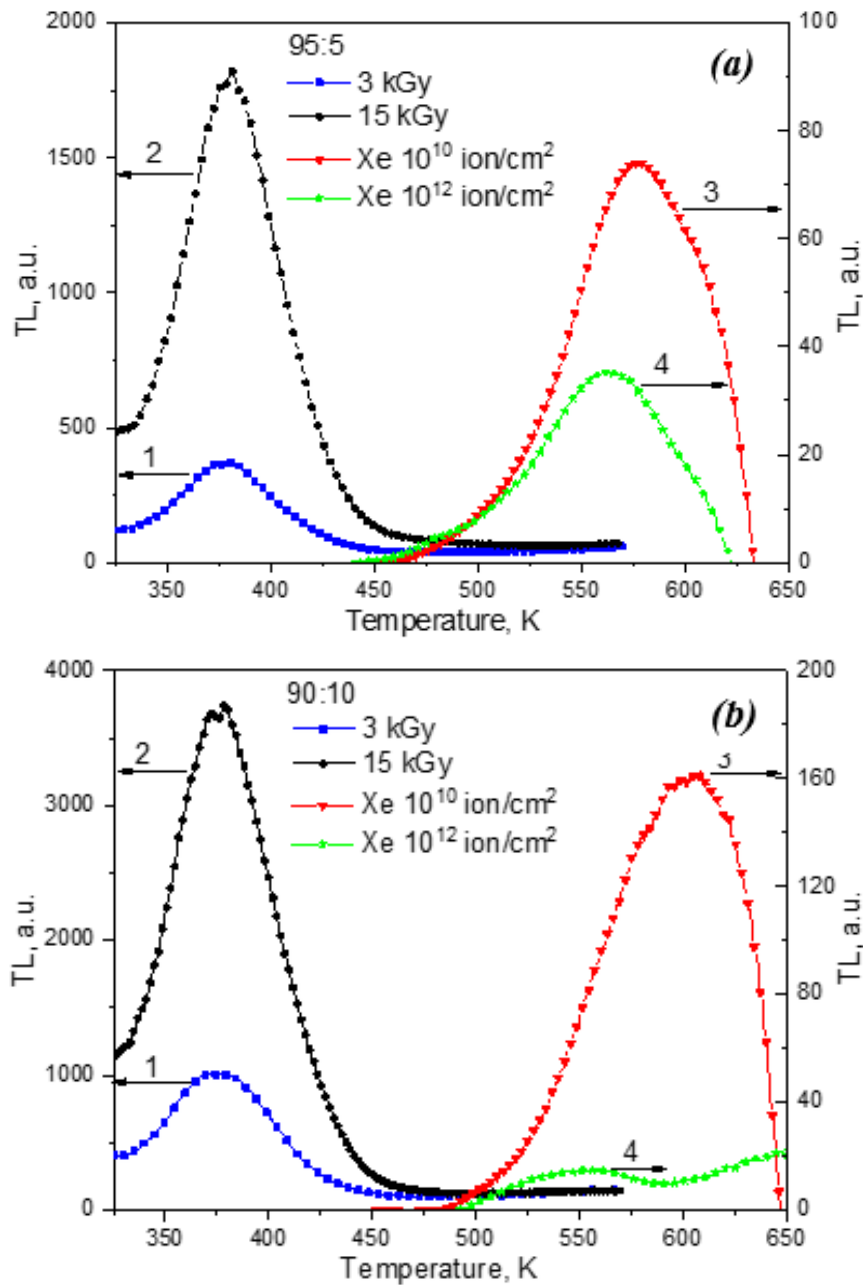


**Figure 4.** TL curves of samples with a concentration of introduced titanium dioxide of 5% (a) and 10% (b), irradiated with electrons at a dose of 3 kGy (1) and 15 kGy (2) and xenon ions with a fluence of  $10^{10}$  ion/cm<sup>2</sup> (3) and  $10^{12}$  ion/cm<sup>2</sup> (4).

Figure 5 shows the TL curves of samples irradiated with ions with different dopant concentrations. It can be seen that the dependence of the TL intensity at 450-650 K on the titanium concentration is, as in the case of PCL, non-monotonic. The maximum intensity is observed for a concentration of introduced titanium dioxide of 1%, which coincides with the results of studying the

PCL spectra. A further increase in the concentration of the dopant causes a decrease in the TL intensity. At a concentration of introduced titanium dioxide of 15%, an increase in the TL signal is observed, as in the case of PCL (Figure 3).

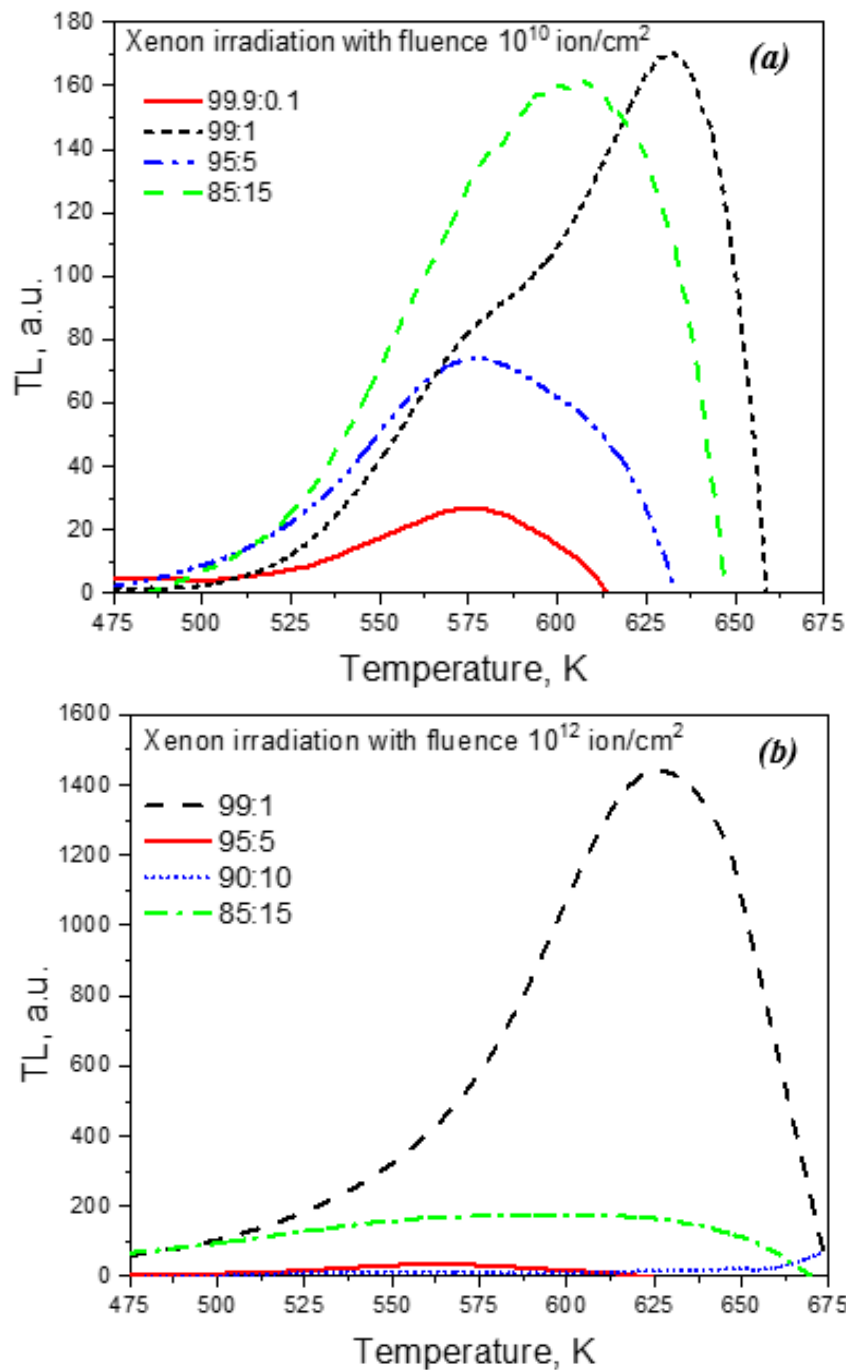


**Figure 5.** TL curves of samples with different dopant concentrations irradiated with xenon ions with a fluence of  $10^{10}$  ions/cm<sup>2</sup> (a) and  $10^{12}$  ions/cm<sup>2</sup> (b).

A nonmonotonic dependence of the PL and PCL intensity on the the concentration of titanium for monoclinic  $\text{ZrO}_2$  samples not subjected to any irradiation was observed in [45]. Moreover, its drop at a high dopant content was associated with concentration quenching of luminescence. The increase in PCL and TL observed by us at the maximum concentrations of introduced titanium dioxide (15%) may be associated with the formation of complex cluster defects, which are responsible for the luminescence band at 2.5 eV. In [45], it was suggested that the nature of this band in monoclinic  $\text{ZrO}_2$  is related to complex vacancy-impurity complexes containing, in particular, titanium ions. A similar relationship may also occur in the samples studied in this work.

#### 4. Conclusions

In this work, zirconium dioxide ceramics with different concentrations of titanium impurity ions were synthesized. It was found that irradiation of samples with high-energy xenon ions leads to a decrease in the PCL intensity at 2.5 eV. In this case, no new emission bands are observed in the PCL spectra. It has been shown that ion irradiation leads to the appearance of a new TL signal at 450-650 K of a non-elementary form, presumably associated with radiation-induced defects that trap charge carriers. Unlike electron irradiation, an increase in ion fluence leads to a decrease in TL intensity. A complex non-monotonic dependence of the PCL and TL intensity on the dopant concentration was discovered, which may be due to the effects of concentration quenching and aggregation of defect centers.

**Acknowledgments:** The work was carried out under the grant of the Ministry of Higher Education and Science of the Republic of Kazakhstan AP09260057 «Luminescence and radiation resistance of synthesized under different conditions micro- and nanostructured compacts and ceramics based on  $ZrO_2$ ».

**Conflicts of Interest:** The authors declare no conflict of interest.

#### References

1. Barry Carter C., Grant Norton M. *Ceramic Materials*. Science and Engineering. Springer New York, 2007; XXII, p. 716. <https://doi.org/10.1007/978-0-387-46271-4>
2. Horowitz Y. S. *Thermoluminescence and Termoluminescent Dosimetry*, 1st edition. CRC Press Taylor and Francis Group. New York 2019; Vol. 3, p. 200.
3. Salah N., Khan Z. H., Habib S. S. Nanoparticles of  $Al_2O_3$ : Cr as a sensitive thermoluminescent material for high exposures of gamma rays irradiations. *Nuclear Instruments and Methods in Physics Research Section B: Beam Interactions with Materials and Atoms* 2011, Vol. 269, 4, 401-404. DOI:10.1016/j.nimb.2010.12.054
4. Frolov E.I. Zvonarev S.V., Moschensky Yu.V., Chesnokov K.Yu., Chukin A.V., Abramov A.V., Churkin V.Yu., Moiseykin E.V., Obvintseva N.V. Synthesis, characterization and luminescent properties of Mg-and Cr-doped alumina ceramics. *AIP Conference Proceedings* 2020, Vol. 2280, 1, 050019. <https://doi.org/10.1063/5.0018319>
5. Zvonarev S. V., Churkin V.Y., Pankov V.A., Chesnokov K.Yu., Chukin A.V., Abramov A.V. Luminescence of alumina ceramic doped with lanthanum under medium-and high-dose irradiation. *Nuclear Instruments and Methods in Physics Research Section B: Beam Interactions with Materials and Atoms* 2020, Vol. 465, 42-46. <https://doi.org/10.1016/j.nimb.2020.01.002>
6. Zvonarev S.V., Frolov E.I., Pankov V.A., Churkint V.Y. Pulse cathodo-and thermoluminescence of alumina ceramic with manganese. *Journal of Physics: Conference Series* 2018, Vol. 1115, 5, 052014. DOI:10.1088/1742-6596/1115/5/052014
7. Zvonarev S.V. et al. Luminescence of impurity and intrinsic defects of Na-doped alumina ceramic. *Nuclear Instruments and Methods in Physics Research Section B: Beam Interactions with Materials and Atoms* 2020, Vol. 471, 53-58. DOI:10.1016/j.nimb.2020.03.023
8. Busuoli G., Lembo L., Nanni R., Sermenghi I. Use of  $BeO$  in routine personnel dosimetry. *Radiation Protection Dosimetry* 1983, Vol. 6, 1-4, 317-320.
9. Tochilin E., Goldstein N., Miller W. G. Beryllium oxide as a thermoluminescent dosimeter. *Health physics* 1969, Vol. 16, 1, 1-7. DOI:10.1097/00004032-196901000-00001
10. McKeever S.W.S. *Thermoluminescence of solids*. Cambridge University Press, London, Ontario, 1985; Vol. 3, p. 390. <https://doi.org/10.1017/CBO9780511564994>
11. Sommer M., Jahn A., Henniger J. A new personal dosimetry system for HP (10) and HP (0.07) photon dose based on OSL-dosimetry of beryllium oxide. *Radiation Measurements* 2011, Vol. 46, 12, 1818-1821. <https://doi.org/10.1016/j.radmeas.2011.07.002>
12. Altunal V. et al. A newly developed OSL dosimeter based on beryllium oxide:  $BeO$ : Na, Dy, Er. *Journal of Luminescence* 2020, Vol. 222, 117140. <https://doi.org/10.1016/j.jlumin.2020.117140>
13. Zahedifar M. et al. Thermoluminescence properties of  $BeO$ : Mg nanoparticles produced by sol-gel method. *Journal of Nanostructures* 2011, Vol. 1, 3, 199-203. DOI:10.7508/jns.2011.03.003
14. Rivera T. et al. Thermal neutron equivalent dose measurements with nanostructured zirconia. *Radiation Effects & Defects in Solids* 2009, Vol. 164, 4, 224-231. DOI:10.1080/10420150802312284
15. Horowitz Y.S., Oster L., Eliyahu I. The saga of the thermoluminescence (TL) mechanisms and dosimetric characteristics of  $LiF$ : Mg, Ti (TLD-100). *Journal of Luminescence* 2019, Vol. 214, 116527. <https://doi.org/10.1016/j.jlumin.2019.116527>

16. Kafadar V.E., Majeed K. F. The effect of heating rate on the dose dependence and thermoluminescence characteristics of  $\text{CaSO}_4$ : Dy (TLD-900). *Thermochimica Acta* **2014**, Vol. 590, 266-269. DOI:10.1016/j.tca.2014.06.015
17. Madhusoodanan U., Jose M.T., Lakshmanan A.R. Development of  $\text{BaSO}_4$ : Eu thermoluminescence phosphor. *Radiation measurements* **1999**, Vol. 30, 1, 65-72.
18. Nieto J.A. Present status and future trends in the development of thermoluminescent materials. *Applied Radiation and Isotopes* **2016**, Vol. 117, 135-142. DOI:10.1016/j.apradiso.2015.11.111
19. Ekdal E., Karala T., Kelemenb A., Ignatovychc M., Holoveyd V., Harmansahe C. Thermoluminescence characteristics of  $\text{Li}_2\text{B}_4\text{O}_7$  single crystal dosimeters doped with Mn. *Radiation physics and chemistry* **2014**, Vol. 96, 201-204. DOI:10.1016/j.radphyschem.2013.10.009
20. Furetta C. et al. Dosimetric characteristics of tissue equivalent thermoluminescent solid TL detectors based on lithium borate. *Nuclear Instruments and Methods in Physics Research Section A: Accelerators, Spectrometers, Detectors and Associated Equipment* **2001**, Vol. 456, 3, 411-417. [https://doi.org/10.1016/S0168-9002\(00\)00585-4](https://doi.org/10.1016/S0168-9002(00)00585-4)
21. Duragkar A., Muley A., Pawar N.R. et al. Versatility of thermoluminescence materials and radiation dosimetry-A review. *Luminescence* **2019**, Vol. 34, 7, 656-665. DOI: 10.1002/bio.3644
22. Cruz-Vázquez C. et al. Thermoluminescence properties of new  $\text{ZnO}$  nanophosphors exposed to beta irradiation. *Optical Materials* **2005**, Vol. 27, 7, 1235-1239. DOI:10.1016/j.optmat.2004.11.016
23. Dhar A., DeWerd L.A., Stoebe T.G. Direct-response ultraviolet thermoluminescent dosimeter. *Medical Physics* **1976**, Vol. 3, 6, 415-417. DOI: 10.1118/1.594259
24. Soliman C. Thermoluminescence behavior of magnesium oxide exposed to gamma and ultraviolet radiations. *Radiation Effects Defects in Solids* **2009**, Vol. 164, 4, 257-265. DOI:10.1080/10420150802349518
25. Dolgov S. et al. Thermoluminescence centres created selectively in  $\text{MgO}$  crystals by fast neutrons. *Radiation protection dosimetry* **2002**, Vol. 100, 1-4, 127-130. <https://doi.org/10.1093/oxfordjournals.rpd.a005828>
26. Salas P. et al. Monoclinic  $\text{ZrO}_2$  as a broad spectral response thermoluminescence UV dosimeter. *Radiation Measurements* **2003**, Vol. 37, 2, 187-190. [https://doi.org/10.1016/S1350-4487\(02\)00174-9](https://doi.org/10.1016/S1350-4487(02)00174-9)
27. Azorín-Vega J.C, Azorin-Nieto J., Garcia-Hipolito M., Rivera-Montalvo T. Thermoluminescence properties of  $\text{TiO}_2$  nanopowder. *Radiation measurements* **2007**, Vol. 42, 4-5, 613-616. DOI: 10.1016/j.radmeas.2007.01.084
28. Zahedifar M., Sadeghi E. Thermoluminescence dosimetry properties of new Cu doped  $\text{CaF}_2$  nanoparticles. *Radiation protection dosimetry* **2013**, Vol. 157, 3, 303-309. DOI: 10.1093/rpd/nct151
29. Wang Z., Zhang J., Zheng G., Liu Y., Zhao Y. The unusual variations of photoluminescence and afterglow properties in monoclinic  $\text{ZrO}_2$  by annealing. *Journal of Luminescence* **2012**, 132, 11, 2817-2821. <https://doi.org/10.1016/j.jlumin.2012.05.039>
30. Aleksanyan E., Kirm M., Feldbach E., Harutyunyan V. Identification of  $\text{F}^+$  centers in hafnia and zirconia nanopowders. *Radiation Measurements* **2016**, 90, 84-89. <https://doi.org/10.1016/j.radmeas.2016.01.001>
31. Paje S.E., Llopis J. Photoluminescence decay and time-resolved spectroscopy of cubic yttria-stabilized zirconia. *Applied Physics A* **1994**, 59, 6, 569-574. <https://doi.org/10.1007/BF00331913>
32. Phatak G.M., Gangadharan K., Pal H., Mittal J.P. Luminescence properties of Ti-doped gem-grade zirconia powders. *Bulletin of Materials Science* **1994**, 17, 2, 163-169. DOI:10.1007/BF02747563
33. Toshihide Ito, Motohiro Maeda, and Kazuhiko Nakamura. Similarities in photoluminescence in hafnia and zirconia induced by ultraviolet photons. *Journal of applied physics* **2005**, 97, 5, 054104. DOI: 10.1063/1.1856220
34. Cong Y., Li B., Yue S., Fan D., Wang X. Effect of oxygen vacancy on phase transition and photoluminescence properties of nanocrystalline zirconia synthesized by the one-pot reaction. *The Journal of Physical Chemistry C* **2009**, 113, 31, 13974-13978. DOI: 10.1021/jp8103497
35. Smits K., Grigorjeva L., Millers D., Sarakovskis A., Grabis J., Lojkowski W. Intrinsic defect related luminescence in  $\text{ZrO}_2$ . *Journal of Luminescence* **2011**, 131, 10, 2058-2062. <https://doi.org/10.1016/j.jlumin.2011.05.018>
36. Carvalho J.M., Rodrigues L.C.V., Hölsä J., et al. Influence of titanium and lutetium on the persistent luminescence of  $\text{ZrO}_2$ . *Optical Materials Express* **2012**, 2, 3, 331-340. <https://doi.org/10.1364/OME.2.000331>
37. Puust L., Kiisk V., Utt K., Mändar H., Sildos I. Afterglow and thermoluminescence of  $\text{ZrO}_2$  nanopowders. *Central European Journal of Physics* **2014**, 12, 6, 415-420. <https://doi.org/10.2478/s11534-014-0456-9>
38. Kiisk V., Puust L., Utt K., Maaroos A., Mändar H., et al. Photo-, thermo- and optically stimulated luminescence of monoclinic zirconia. *Journal of Luminescence* **2016**, 74, 49-55. [doi.org/10.1016/j.jlumin.2015.12.020](https://doi.org/10.1016/j.jlumin.2015.12.020)
39. Salas-Juarez Ch.J., Burruel-Ibarra S.E., Gil-Tolano M.I., Perez Rodriguez A., Romo-Garcia F. et al. Persistent luminescence of  $\text{ZrO}_2:\text{Tb}^{3+}$  after beta particle irradiation for dosimetry applications. *Journal of Luminescence* **2023**, 257, 119712. <https://doi.org/10.1016/j.jlumin.2023.119712>
40. Lokesha H.S., Chithambo M.L., Chikwembani S. Thermoluminescence of monoclinic  $\text{ZrO}_2$ : Kinetic analysis and dosimetric features. *J. Lumin.* **2020**, 218, 116864. <https://doi.org/10.1016/j.jlumin.2019.116864>
41. Bettinali C., Ferrarese G., Manconi J.W. Thermoluminescence of  $\text{ZrO}_2$ . *J. of Chem. Phys.* **1969**, 50, 9, 3957-3961. <https://doi.org/10.1063/1.1671655>

42. Iacconi P., Lapraz D., Caruba R. Traps and emission centres in thermoluminescent  $\text{ZrO}_2$ . *Phys. stat. sol. (a)* **1978**, *50*, 275-283. <https://doi.org/10.1002/pssa.2210500133>
43. Costantini J. M., Beuneu F. Color center annealing and ageing in electron and ion-irradiated yttria-stabilized zirconia. *Nucl. Instrum. Methods Phys. Res. B* **2005**, *230*, 1-4, 251-256. <https://doi.org/10.1016/j.nimb.2004.12.050>
44. Costantini J. M., Beuneu F., Fasoli M., Galli, A., Vedda, A., Martini, M. Thermo-stimulated luminescence of ion-irradiated yttria-stabilized zirconia. *J. Phys. Condens. Matter* **2011**, *23*, 11, 115901. <https://doi.org/10.1088/0953-8984/23/11/115901>
45. Nikiforov S.V., Menshenina A.A., Konev, S. F., The influence of intrinsic and impurity defects on the luminescent properties of zirconia. *J. Lumin.* **2019**, *212*, 219-226. <https://doi.org/10.1016/j.jlumin.2019.03.062>
46. Ananchenko D.V., Nikiforov S.V., Sobyanyin K.V., Konev S.F., Dauletbekova A.K., Akhmetova-Abdik G., Akilbekov A.T., Popov A.I. Paramagnetic Defects and Thermoluminescence in Irradiated Nanostructured Monoclinic Zirconium Dioxide. *Materials* **2022**, *15*, 8624. <https://doi.org/10.3390/ma15238624>
47. Ananchenko D.V., Nikiforov S.V., Kuzovkov V.N., Popov A.I., Ramazanova G.R., Batalov R.I., Bayazitov R.M., Novikov H.A. Radiation-induced defects in sapphire single crystals irradiated by a pulsed ion beam. *Nuclear Inst. and Methods in Physics Research B* **2020**, *466*, 1-7. <https://doi.org/10.1016/j.nimb.2019.12.032>

**Disclaimer/Publisher's Note:** The statements, opinions and data contained in all publications are solely those of the individual author(s) and contributor(s) and not of MDPI and/or the editor(s). MDPI and/or the editor(s) disclaim responsibility for any injury to people or property resulting from any ideas, methods, instructions or products referred to in the content.